communications earth & environment

Article

A Nature Portfolio journal

https://doi.org/10.1038/s43247-025-02833-w

Land use impacts the environmental benefits of wind energy farms in China

Check for updates

Kang Xu [1], Hanwen Zhu [2,3], Shuai Zhang [2,3], Mingming Wang [2,3], Wei Li [4], Wenji Zhou [5], Shuangcheng Li [6], Zhou Shi [2,3] & Jinfeng Chang [2,3] ✉

Wind energy plays a vital role in meeting rising electricity demand and climate goals, but its land-use footprints from vegetation removal, construction, and road sprawl may overestimate greenhouse gas (GHG) mitigation benefits. Here we used life cycle assessment (LCA) to explore the land-use impacts on GHG emissions and energy performance for three typical wind farms located in forest, grassland and desert ecosystems. We incorporated vegetation/soil removal during the installation stage, and the loss of additional carbon sink capacity during the operation and maintenance stage. Land-use change (LUC) contributed 37.9% of the life cycle emissions for the forest farm, while much lower for the grassland and desert farm (4.3% and 1.2%, respectively). Grassland deployment offered a triple win with highest energy return, lowest land-use intensity, and lowest GHG emissions. With mitigation measures, all farms achieved low emission intensity (below 5 g CO_2-eq kWh^{-1}), greatly reducing land-use and ecosystem-based emission intensity differences.

China has the largest electricity sector in the world with an installed capacity of 2.2 TW (Tera Watt) and a total generation of 7521 TWh (Tera Watt · hour) in 2020[1]. Meanwhile, greenhouse gas (GHG) emissions from China's electricity sector have risen sharply and contributed 47% (around 5.4 Gt) of the national total GHG emissions in 2020[2]. To tackle climate change and improve the sustainability of its socio-economic development, China's government pledged in 2019 to "achieve peak emissions before 2030 and carbon neutrality before 2060". This pledge requires strong decarbonization of China's electricity sector, including increasing renewable power generation, phasing out conventional coal-fired power plants, and increasing the flexibility of power grids[3].

Wind energy provides substantial benefits for achieving climatic goals. Currently, the GHG emission intensity of China's wind energy is 19.88 g CO_2-eq kWh^{-1}, providing 98% mitigation effect compared to fossil fuels[4]. With the world's fastest wind power growth, China accounted for 56% of global new installation in 2020[5]. Wind energy is growing rapidly and will continue to grow to meet the increasing electricity demand and displace existing fossil-based generation. It is estimated that the wind power generation of China will reach 4860 TWh and 5760 TWh in 2050 under 2 °C and 1.5 °C scenario, accounting for 37% and 40% of the total electricity demand, respectively[6]. However, wind farms require more land than other energy sources[7–9], with turbines typically spaced 7–15 rotor diameters apart[10]. The rapid and large-scale deployment of wind energy requires substantial land areas, creating significant land-use footprints through vegetation removal and on-site construction of wind facilities[11].

Continental-scale occupation of wind farms causes non-negligible impacts on heat and moisture fluxes[12,13] and global carbon cycle[14], induces habitat deforestation/destruction[11] and leads to increasing threats to biodiversity[15,16]. However, life cycle assessment (LCA), the widely employed method in evaluating the GHG emissions associated with wind energy facilities[17], often overlooks the critical effects from land-use change (LUC). Vegetation removal reduces biomass storage and further causes soil carbon losses. The construction of a single wind turbine in grassland damaged approximately 3000 m^2 of pasture land[18]. Remote-sensing data also revealed reductions in the vegetation index after wind farm installation, indicating that wind energy deployment within natural ecosystems inhibits vegetation growth and productivity[19,20]. Furthermore, on-site construction of impermeable surfaces, such as turbine foundations and road sprawl, will inhibit the carbon input. Pekkan et al.[21] found that a 466 ha wind farm significantly decreased soil organic carbon by 18 kt over ten years. For energy forms with higher land-use intensity than wind, studies still report non-negligible LUC emissions. For example, for unconventional oil and gas, LUC induced emissions accounted for 4% of the life cycle emissions[22]. For

[1]Jiangsu Key Laboratory for Recognition and Remediation of Emerging Pollutants in Taihu Basin, School of Environmental Science and Engineering, Wuxi University, Wuxi, China. [2]Zhejiang Key Laboratory of Agricultural Remote Sensing and Information Technology, Zhejiang University, Hangzhou, China. [3]College of Environmental and Resource Sciences, Zhejiang University, Hangzhou, China. [4]Ministry of Education Key Laboratory for Earth System Modeling, Department of Earth System Science, Tsinghua University, Beijing, China. [5]Department of Energy Economics, School of Applied Economics, Renmin University of China, Beijing, China. [6]College of Urban and Environmental Sciences, Peking University, Beijing, China. ✉e-mail: changjf@zju.edu.cn

renewables like solar photovoltaics, neglecting changes of carbon flux will result in an underestimation of emissions by 25–51%[23]. GHG emissions of biofuels from LUC even produce much more CO_2 than GHG reduction they provide by replacing traditional fossil fuels[24], especially for intensified production[25]. Therefore, it is imperative to integrate LUC induced GHG emissions from wind energy. The neglection of the carbon losses from LUC leads to incomplete and falsely estimation of life cycle GHG emissions and overestimation of wind's climate change mitigation potential compared to other energy sources.

In this study, we selected three typical wind farms located in forest, grassland and desert ecosystems to explore their life cycle GHG emissions and energy performance, as well as the contribution of LUC impact. We developed a comprehensive LCA framework integrating the effects of vegetation and soil destruction by wind farm deployment. The objectives of this study are (1) to estimate the contribution of emissions from LUC to life cycle emissions and energy efficiency of wind farms deployed in different ecosystems; (2) to quantify LUC emission contributions to life cycle emissions and energy efficiency across ecosystems; and (3) to propose feasible site-planning methods balancing emission mitigation, land use, and energy efficiency based on scenario analyses.

Results

Land-use impacts on the life-cycle GHG emissions

The results showed substantial carbon losses caused by LUC for wind farm installation, operation and maintenance, especially in forest and grassland ecosystems. In the forest wind farm (FWF), biomass carbon loss was 243.88 t C turbine^{-1} in the FWF location, which dominated the carbon losses (Fig. 1). Vegetation removal also resulted in a loss of additional carbon sink capacity (LASC) of 23.54 t C turbine^{-1}. Soil organic carbon (SOC) losses were 28.01 t C turbine^{-1} over 20 years due to impermeable surfaces inhibiting carbon input. The large carbon losses in the FWF were determined by its greater land-use footprint (44.3 m^2 GWh^{-1}; Table 1). In the grassland wind farm (GWF), biomass carbon loss (9.95 t C turbine^{-1}) was a larger source of carbon losses than SOC reduction (5.27 t C turbine^{-1}). Minimal carbon losses (5.04 t C turbine^{-1}) occurred in the desert wind farm (DWF) location due to low LASC, low soil carbon content and biomass in the desert ecosystem. Overall, the total carbon losses caused by the deployment of FWF were more than 13 times those in the GWF and nearly 60 times those in the DWF (Fig. 1).

LUC induced emissions comprised 37.9% of total life cycle emissions (2865 t CO_2-eq turbine^{-1}) for the FWF. For the GWF, the emissions during the installation and operation stage were underestimated by 27.4% if ignoring carbon losses (Fig. 2), while 4.3% of the life cycle emissions were contributed by LUC. In contrast, the LUC induced emissions accounted for only 1.2% of the life cycle emissions for the DWF (1520 t CO_2-eq turbine^{-1}). Ignoring land-use impacts substantially underestimates onshore wind energy emissions, especially in high-biomass ecosystems like forests. LCAs that overlook land-use impacts likely overestimate wind power's climate mitigation potential.

The FWF had much higher life cycle emission intensity (emissions per unit of electricity generation) than GWF and DWF (Table 1). Decomposition of emission intensity differences between the FWF and GWF showed LUC as the primary source (62%; Fig. 3a), with wind energy potential and turbine specifications explaining only 12% and 25% of the variance, respectively. For the FWF-DWF comparison, LUC remained the dominant source of difference (87%). These results indicate LUC alone causes considerable variations in the life cycle emissions of wind farms installed in diverse ecosystems, independent of factors like wind potential or turbine type differences.

Land-use impacts on energy performance

The power generation intensity of the FWF, the GWF and the DWF selected in this study was 56.9, 61.8 and 52.8 GWh MW^{-1}, respectively (Table 1). The energy return on investment (EROI) was the highest in the GWF (26.0), followed by the DWF (16.9) and the FWF (14.7, Fig. 4; Table 1). That means the GWF could achieve the greatest economic benefits, and a unit of energy input can produce 26.0 times of electric output throughout the entire life of this wind farm. The energy payback of the GWF was the fastest, which took less than 1 year, while the energy payback time (EPT) was 16 months and 14 months for the FWF and DWF, respectively (Table 1).

Despite substantial differences in power generation and energy performance between the three wind farms, land-use contributed marginally to the changes in life cycle energy input (Figs. 2, 3). For the FWF, timber transportation increased energy input by about 0.1%. For the GWF and DWF, land-use energy costs could be negligible (<1%). EROI pairwise difference analysis also showed marginal LUC contributions (<1%). Wind turbine was another important factor affecting energy performance, accounting for 25% of EROI difference between the FWF and GWF (Fig. 3b). Wind potential contributed minimally to energy performance (Fig. 3b and Supplementary Fig. 1).

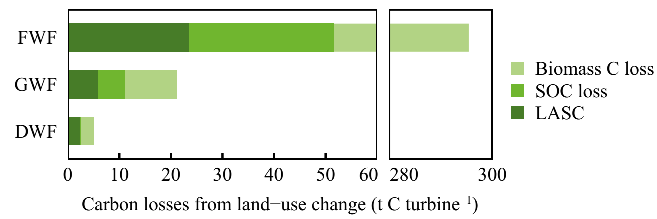

Fig. 1 | Carbon losses per turbine caused by LUC of wind farms in different ecosystems. Carbon losses include biomass C loss, soil organic carbon (SOC) loss, and loss of additional sink capacity (LASC).

Table 1 | Life cycle performance of the three wind farms

	FWF	GWF	DWF
Land Conversion per MW (ha MW^{-1})	0.25	0.19	0.42
Land-use footprint (m^2 GWh^{-1})	44.3	30.1	77.8
GHG emissions (t CO_2-eq turbine^{-1})	2865	1795	1520
Emission intensity (g CO_2-eq kWh^{-1})	33.6	14.5	19.2
Energy consumption (TJ turbine^{-1})	20.9	17.1	16.9
Power generation (GWh turbine^{-1})	85.3	123.6	79.2
Generation Intensity (GWh MW^{-1})	56.9	61.8	52.8
Energy payback time (month)	16	9	14
Energy return on investment	14.7	26.0	16.9

Sensitivity analysis of impact factors

The sensitivities of the wind power potential to the most important parameters are shown in Fig. 4. Emission intensity and EROI were highly sensitive to capacity factor and lifetime. The substantial variation of emission intensity caused by capacity factor reflected the diverse wind potential across geographical locations, particularly for forest-located farms. Due to ecosystem variations in vegetation coverage and SOC content across ecosystems, emission intensity of the FWF was also sensitive to land-use area and ecosystem type (Fig. 4a). For the FWF, the most primary factor contributing to variations in GHG emission intensity for the FWF is the land-use area. However, for the GWF and the DWF, the emission intensity was less sensitive to the variation of land-use. While the emission intensity of our specific case-study FWF (33.59 g CO_2-eq kWh^{-1}) was higher than the mean value calculated for all forest-located wind farms in China (28.27 ± 3.55 g CO_2-eq kWh^{-1}), it should be noted that the mean GHG emission intensity for wind farms located in forests was demonstrably higher than the mean emission intensities for wind farms in deserts (19.43 ± 0.20 g CO_2-eq kWh^{-1}, $p < 0.05$) and grasslands (14.65 ± 0.38 g CO_2-eq kWh^{-1}, $p < 0.05$). The Cement and the Steel & Iron were also important contributors with varying

Fig. 2 | Life cycle greenhouse gas emissions and energy consumption of the three wind farms. Open circles represent the contributions of different life cycle stages to the total energy consumption (left column) and GHG emissions (right column) for three types of wind farms: **a** FWF, **b** GWF, and (**c**) DWF. The life cycle stages include manufacturing, transportation, installation, operation and maintenance, and disassembly and disposal. The contributions from land-use change are highlighted by green boxes.

impacts on the emission intensity and EROI among the wind farms. Variations in the Other materials, Transport distance, and Curtailment rate generally had minimal effects on GHG emission intensity and the EROI in most cases.

Benefits from different mitigation measures

We found that implementing all measures (the Combination of all 7 scenarios including $S_{lifetime}$, $S_{advanced}$, S_{clean}, $S_{recycling}$, S_{land}, $S_{curtailment}$ and S_{6MW}) would reduce emission intensity by 89% for the FWF (i.e., reach 3.67 g CO_2-eq kWh^{-1}), 83% for the GWF (i.e., reach 2.45 g CO_2-eq kWh^{-1}), and 78% for the DWF (i.e., reach 4.21 g CO_2-eq kWh^{-1}; Fig. 5). Under the Combination scenario, wind farms across different regions achieved extremely low and similar emission intensity, indicating excellent emission reduction potential. For the GWF and DWF, the S_{6MW}, $S_{advanced}$, and $S_{lifetime}$ led to significant emission reductions. In contrast, $S_{recycling}$, and S_{land} together proved the most effective mitigation measures for the FWF, due to the greater land-use intensity and associated carbon losses in forest ecosystems. Regardless of the deployment location, the combination of scenarios substantially increased EROI across all wind farms: 487% for the FWF, 426% for the GWF, and 377% for the DWF (Fig. 5). The S_{6MW}, $S_{advanced}$, and $S_{lifetime}$ each enhanced EROI across regions. Notably, under the S_{6MW}, EROI increase for the DWF was lower than for the FWF and GWF. This resulted in slightly lower EROI of the DWF versus the FWF in the Combination scenario—contrasting with Baseline results.

Discussion

Impacts of LUC on LCA results

Land requirements of onshore renewables impose apparent constraint on future large-scale deployment[23,26]. However, few studies link land-use impacts to wind energy's emission mitigation potential or other socio-economic benefits of wind energy. We developed a comprehensive LCA framework integrating the effects of vegetation removal, soil destruction and LASC caused by LUC due to wind farm deployment, and explored these effects on GHG emissions and energy performance. Our results highlight that LUC induced GHG emissions could play a vital role in total emissions. Ignoring the LUC induced emissions may underestimate emissions by one-third emission for forest-located wind farms. When excluding the impacts of land-use, our results (13.90–20.86 g CO_2-eq kWh^{-1}) align with previous studies on China's wind energy (19.88 g CO_2-eq kWh^{-1})[4]. Therefore, omitting LUC effects substantially overestimates GHG emission mitigation potential and provides misleading messages policy guidance for energy mix optimization.

Compared to its sizable GHG emission impact, LUC marginally effects on energy performance metrics of wind farms such as EROI. Our analysis showed that land-use impact like vegetation removal and soil disruption contributed <1% to installation and operational energy inputs. This contrasts sharply with LUC's considerable emission contributions, particularly in forest and grassland ecosystems. We propose that LUC induced emission changes should be regarded as a critical ecological indicator in future wind

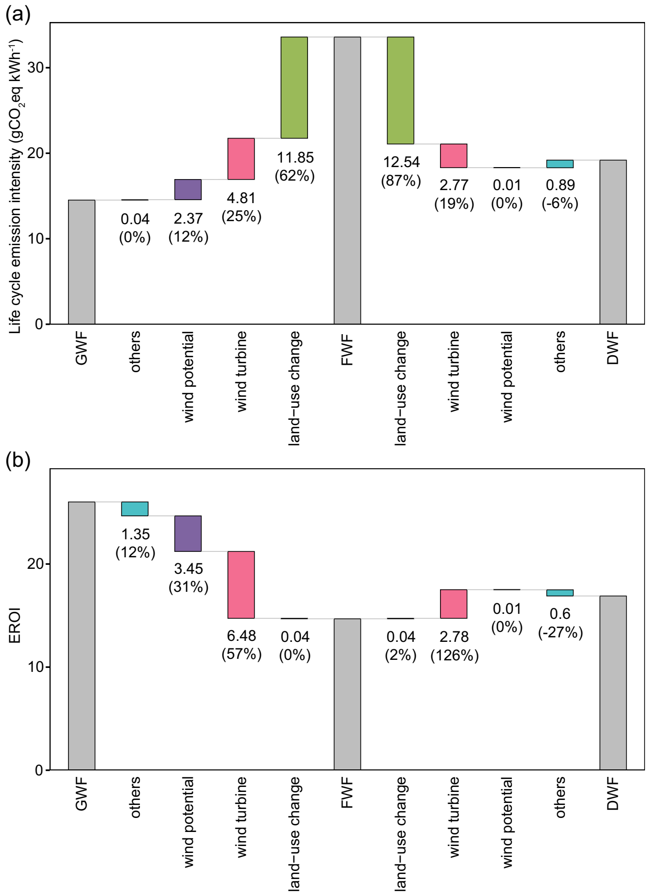

Fig. 3 | Key drivers of variations in environmental and energy performance. The drivers contributing to the differences in (**a**) GHG emission intensity and (**b**) EROI among different wind farms include land-use change, the type of wind turbine, local wind potential, and other relevant factors. The numbers under the suspended bars indicate the effect of the single factor, while the numbers in parentheses indicate the contributions in percentage.

site selection, while the impacts of LUC on economic advantages of wind energy are negligible.

In addition to generating extra GHG emissions, LUC from wind farm deployment might threaten local habitats of wildlife and alter the ecosystem functioning. Though directly impacted lands account for a small fraction of total landscape area (1–4%)[11], permanently occupied zones significantly reduce habitat quality and limit installed capacity density[27]. Pursuing higher energy efficiency necessitates dedicated land buffers from habitations, drastically expanding land-use footprint (increasing landscape land-use intensity). Larger inter-turbine spaces improve energy efficiency but expand the indirect climate impact areas. The divergence between direct land-use footprint and landscape land-use provides opportunities for joint human-environment synergies such as energy self-sufficient livestock farms[28] or plant factories[29]. Therefore, energy efficiency-land requirement tradeoffs highlight synergies between renewables with agriculture production. Pursuing these synergies, alongside habitat-conscious siting and compact land-use footprints, can help offset potential land-use conflicts between wind power and conservation priorities.

Mitigation potential and energy performance under different scenarios

A key motivation for rapidly upscaling wind energy is displacing higher-emission fossil power generation. However, unmitigated wind farm emissions, especially from LUC, can erode the expected climate benefit. Our baseline emission intensity of wind farms built in areas with high biomass and low wind resources (e.g., 33.59 g CO_2-eq kWh^{-1} for the FWF in this study) even exceeded hydropower (26 g CO_2-eq kWh^{-1}) and approached bioenergy (45 g CO_2-eq kWh^{-1})[30], conflicting with decarbonization priorities.

Recycling removed forest biomass for wood production specifically addressed LUC induced emissions, reducing life cycle GHG emissions by 28% (9.53 g CO_2-eq kWh^{-1}). This compensates for the highest LUC burden, at an economic expense (−8% efficiency). Investors will likely employ such nature-based mitigation only if revenue and emission reductions outweigh losses. Meanwhile, extending the service lifetime of the turbines to 25.4 years or adopting advanced manufacturing technology can effectively reduce emissions while increasing returns. It is noted that the lifetime of Denmark's wind turbines is relatively short for modern turbines, making our results conservative estimates of emission reduction benefits for lifetime extension and may underestimate the LUC induced GHG emissions in the $S_{lifetime}$. For all wind farms, extending lifetime, improving manufacturing, and deploying next-generation turbines can reduce emissions and increase efficiency - favorable options across regions. Further performance improvements are foreseeable post-repowering.

The combined measures dramatically increased EROI by 377% – 487%. Wind no longer necessitates inherent trade-offs between climate mitigation and economic viability. With holistic advancement pathways targeting key life cycle stages, from manufacturing to decommissioning, win-win climate and economic outcomes are achievable even for established renewable options.

Where to build wind farms?

Beyond quantifying land-use impacts, an objective of this work was exploring ecosystem contexts balancing land-use, climate goals and economic returns. Our LCA results revealed a triple win for the GWF with highest EROI, lowest land-use intensity, and lowest GHG emissions. Our results contradict that of Gao et al.'s[31], who highest emission intensity for grassland farms and lowest for Gobi farms. This inconsistency stems from the differences in wind potential and inadequate consideration of LUC induced emissions are the major reasons for the inconsistency between the two studies, because LUC and wind turbine type explain emission reduction variations across farms. Even excluding impacts of wind turbine type and considering both climate and energy benefits, grasslands are more suitable deployment sites. Despite the limitation of incomplete life cycle inventory data, our initial focus on a single grassland farm expanded through decomposition (Fig. 3) and sensitivity analyses (Fig. 4), incorporating 140 Chinese grassland farms' geographic coordinates (key emission drivers), yielding a final output of 14.65 ± 0.38 g CO_2-eq kWh^{-1} (Fig. 4b). This result is notably lower than that of China's forest wind farms (28.27 ± 3.55 g CO_2-eq kWh^{-1}) and comparable to Gobi wind farms (19.43 ± 0.20 g CO_2-eq kWh^{-1}). Grassland wind farms exhibited a higher EROI (20.62 ± 0.05) compared to that of desert wind farms (16.52 ± 0.03), suggesting superior energy efficiency (Fig. 4b).

Prioritizing deserts exploits large wind potential via sprawling installations, though reasonable capacity factors may enlarge inter-turbine spaces. The cost of installation planning in remote areas cannot be ignored (Fig. 2) and may potentially damage fragile arid ecosystems. Given desert ecosystems' vulnerability, low biodiversity, and low resistance stability, the negative impacts on biodiversity and socio-ecological resources weaken the ecosystem services caused by relatively high land-use footprint of many renewable facilities should not be ignored[32]. Desert species exhibit limited climate resilience and restoration potential[33]. Although direct habitat destruction is minor relative to landscape scales, ecosystem fragility heightens conservation concerns.

High turbulence in and around forests reduces power generation and shortens the lifetime of wind turbines[34]. Meanwhile, clearing vegetation incurs land-use emissions via biomass and soil carbon losses (1.35 kt CO_2-eq $turbine^{-1}$ in this study), which led to the extremely high emission intensity. The greater uncertainty in power generation from wind farms located in forests compared to those in grasslands and deserts reflects the higher variance of wind resource in forest sites (Fig. 4a). Additionally, 2% of the forest wind farms (3 out of 128) operate at a capacity factor of less than

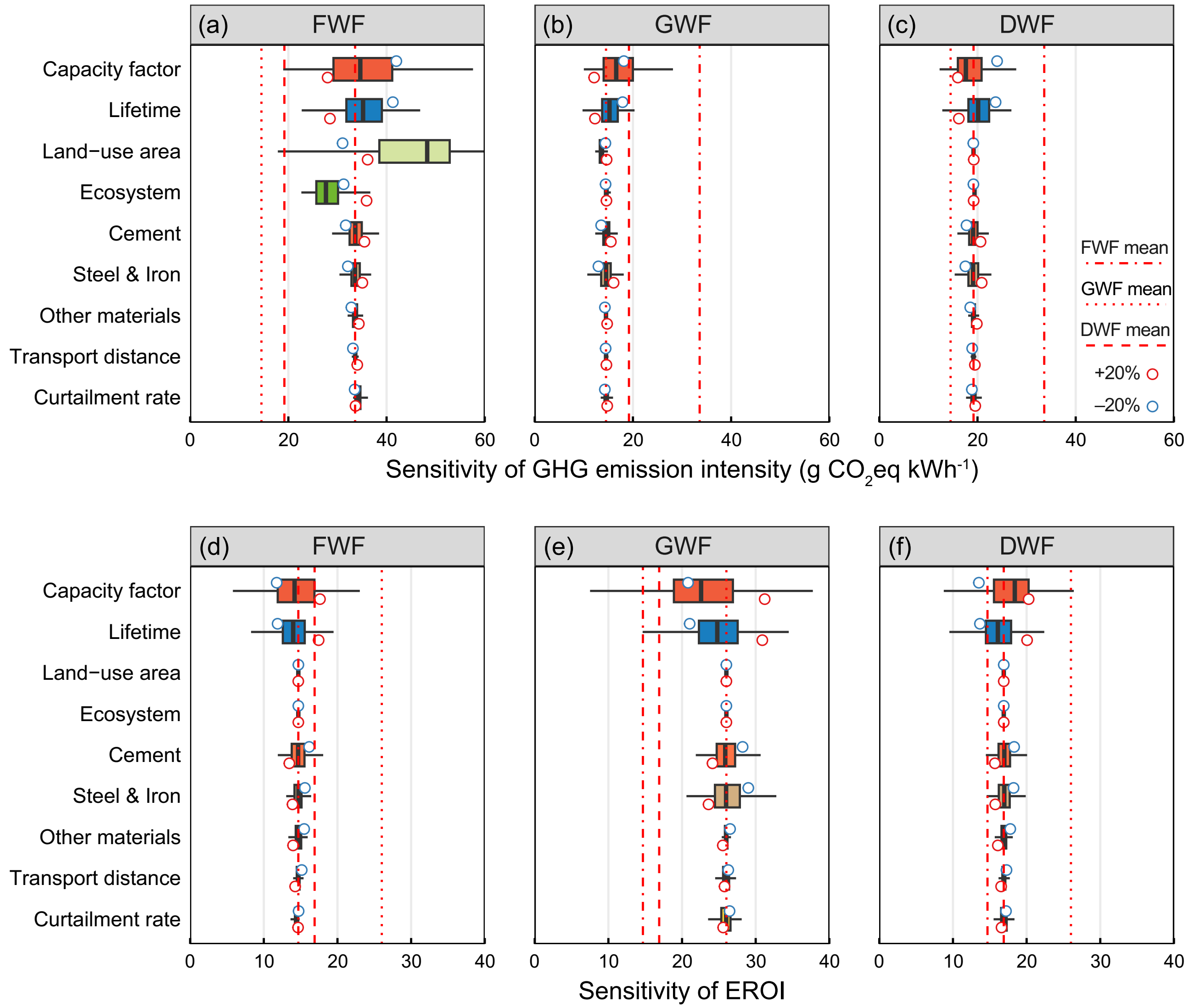

Fig. 4 | Sensitivity analysis of the LCA results given ± 20% variations and the Monte Carlo simulation of different input parameters. The boxplots represent the variations in the GHG emission intensity of (**a**) FWF; **b** GWF; **c** DWF and the EROI of (**d**) FWF; **e** GWF; **f** DWF in relating to the variations in capacity factor, lifetime, occupied area, cement use, steel & iron use, other material use, and transport distance across the 128 forest, 141 grassland, 124 desert wind farms within China. The mean values for FWF, GWF, and DWF are represented by dotted-dashed lines, dotted lines, and dashed lines, respectively. Red and blue circles indicate the increase (+20%) and decrease (−20%) of input parameters, respectively.

0.2 even after applying bias-correction to the wind speed data (Eqs. (1), (2)). This high variability underscores the inherent challenge of predicting power generation in such complex terrain from global climate data. Therefore, considering the environmental impacts and energy efficiency, deploying wind farms in forests with low wind speed and high biomass faces greater risks. Selecting forest areas that need thinning and utilize the existing network of forestry roads for the development of the wind farm site are prior measures to reduce the negative impacts of forest wind farms[35].

Siting wind facilities on agricultural or marginal land, contaminated sites or in the built environment rather than in undisturbed natural systems might decrease unintended consequences of wind energy development. Specifically on agricultural land, wind energy deployment is often compatible with agriculture and allows power generation and crop production to coexist on the same landscape. Empirical studies consistently show that co-locating wind infrastructure with farming operations induces minimal land-use change[36,37], Emerging evidence even suggests certain configurations may enhance neighboring crop yields through microclimate modification[38]. The Chinese government actively promotes wind energy integration in agricultural areas, such as “Thousands of townships and tens of thousands of villages harnessing the wind program”, to advance rural energy’s green, low-carbon transformation and boost farmers’ incomes[39,40]. However, siting wind turbines in rural areas that include a mix of homes and smallholder farms can also be challenge given the fact that building turbines would require permission and lease agreements with multiple landowners. In addition, attention needs to be paid to turbines located in built environment due to the noise and shadow-clicker which promote annoyance and stress effects on people living nearby[41,42]. When these socio-technical challenges are adequately addressed, agricultural areas represent a high-priority avenue for sustainable wind development that balances energy goals with land stewardship.

Limitations and implication

Our work emphasizes that incorporating ecosystem-specific LUC induced emissions within LCA boundaries significantly affects climate impact assessment for wind siting contexts. However, consideration of potential effects of wind farms on surrounding vegetation and wildlife habitat at broader landscape scales need to be considered. Some studies indicated wind facilities may inhibit vegetation growth at regional scales based on remote-

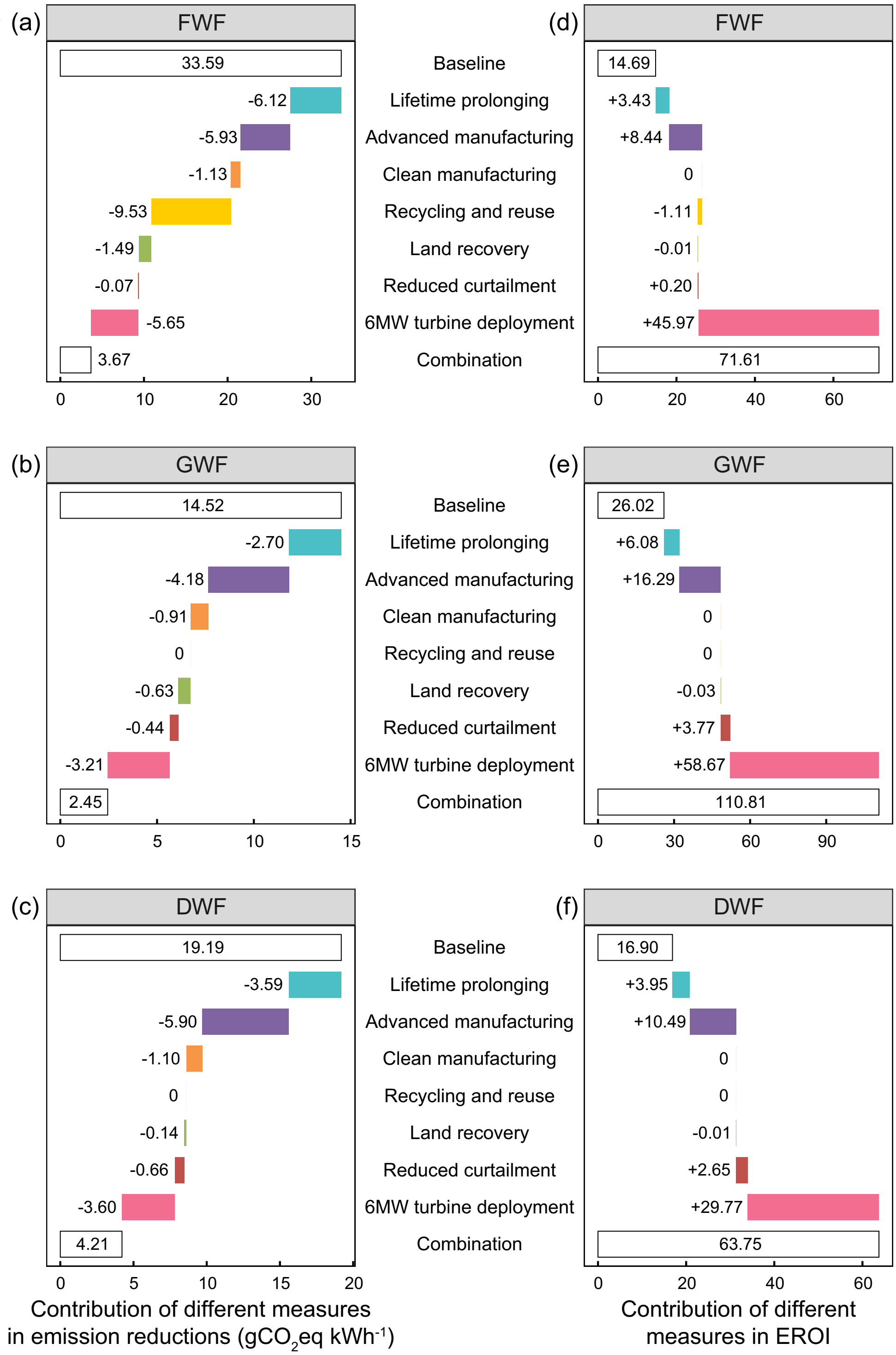

Fig. 5 | Scenario analysis for GHG mitigation and EROI enhancement from different measures. **a**–**f** the contributions of various mitigation measures for reducing the GHG emissions (**a**–**c**) and increasing the EROI (**d**–**f**) of the three wind farm types: FWF (**a**, **d**), GWF (**b**, **e**), and DWF (**c**, **f**). The values within the open black squares indicate the GHG emissions and EROI of the wind farms under baseline scenario (Baseline) or with all mitigation measures combined (Combination), while the numbers adjacent to the colored bars indicate the individual effects of each mitigation measure.

sensing observation[19,20], while others reported neutral[43,44] or positive effects[45,46], due to differences in community structure and microclimate changes induced by wind wakes. This depends on long-term remote sensing monitoring or field experiments to explore the response of vegetation to climate change across the entire life cycle. Due to incomplete life cycle inventory data, our study focused on three typical wind farms. However, decomposition and sensitivity analyses considering the China's geographical variation of wind farms yielded consistent results. In future, more openly available wind turbine inventory data will be essential to more accurately assess the contribution of LUC.

We encourage future studies to combine the LCA methodology with quantitative ecological models (such as species-area curves, population models, species distribution models, and collision risk models) to quantify impacts of wind farm size and land-use footprint on ecosystems, including plant richness, population size, habitat quality and collision risk[47,48]. The indirect impacts on landscape areas for habitation should also be quantified. LUC may not be the primary source of conflict between wind energy performance and climate benefits; however, it will be a factor in the conflict between ecological impacts and climate benefits. Modeling the emission intensity and energy efficiency as well as the impacts of carbon sink

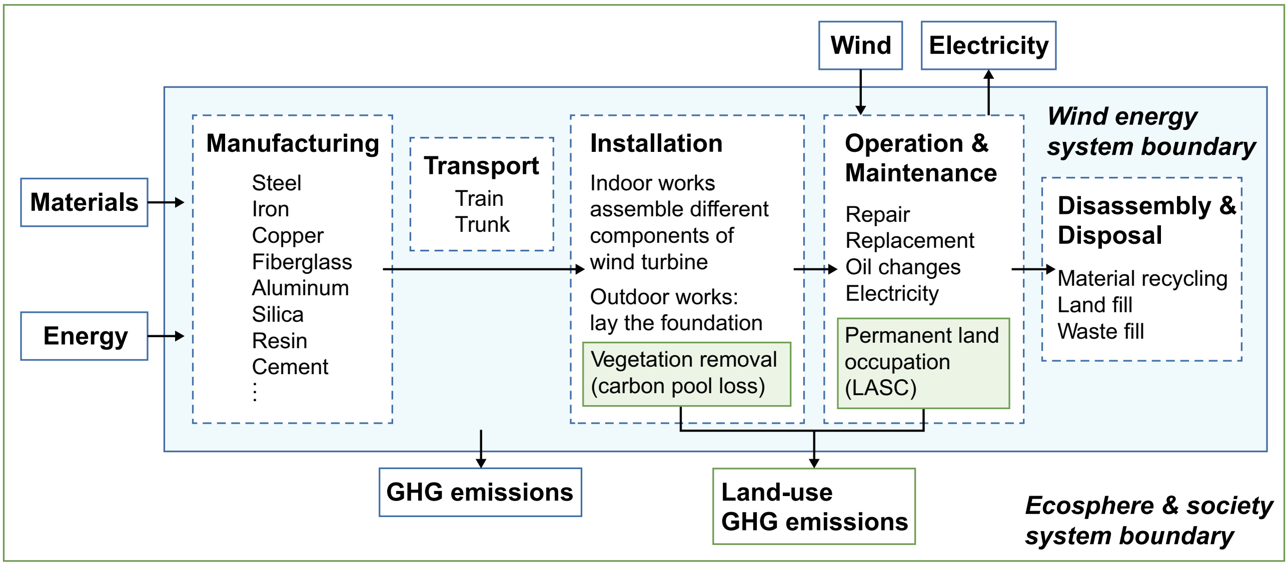

Fig. 6 | System boundaries covering all life stages of wind power in this study.

Table 2 | The selected wind farms in this study

Name	Province	Ecosystem type	Longitude (°E)	Latitude (°N)	Total installed capacity (MW)
Shaobaishan wind farm (FWF)	Heilongjiang	forest	129.69	47.76	49.5
Dongshan wind farm (GWF)	Inner Mongolia	grassland	117.94	42.64	200
Guazhou Qiaowan wind farm (DWF)	Gansu	desert	95.84	40.65	201

potential, habitat alterations, disturbance, and collisions within an integrated LCA framework can balance trade-offs between climate change benefits (larger wind turbines and more land) and biodiversity threats (small turbines and less land) from wind power development.

Methods

LCA framework

In this study, we developed a comprehensive LCA framework to quantify the GHG emissions resulted from LUC and to evaluate the contribution of LUC impacts to the overall climate and energy performance of wind power. The environmental and energy indices include GHG emission intensity, land-use footprint, energy consumption, EROI and EPT. The functional unit is defined as 1 kWh of electricity generated. The system boundary of the wind farm life cycle in this study includes five stages: manufacturing, transportation, installation, operation and maintenance, and disassembly and disposal (Fig. 6). The assumed baseline lifetime was 20 years.

In addition to indoor and outdoor works, the installation stage further involves land-use alterations—impermeable surfacing, vegetation clearance, soil disturbances - triggering GHG emissions from biomass and SOC losses, and foregone carbon sequestration[19,21,49]. These impacts are accounted for in our LCA framework, including carbon storage losses during installation and lost sink capacity during operation (the green boxes in Fig. 6). The detailed information of the LCA framework see Supplementary Methods 1.1.

Site description

Three quarters of turbines in China located in natural areas including grassland (37.4%), desert (20.6%) and forest (18.0%; Supplementary Fig. 2a), while in the United States, over half of wind farms were sited in cropland (Supplementary Fig. 2b). According to the distribution of China's wind energy, three representative wind farms, sited in forest, grassland and desert, were selected. Table 2 lists the basic information of each wind farm. Detailed information of the three wind farms sees Supplementary Table 1. The resolution of remote sensing images of cities provided by Google Earth is up to 0.61 m, which make it possible to identify the boundary and land occupation of artificial facilities by visual interpretation[50]. We used high-resolution digital photographs to distinguish pre-construction and post-construction roads using on-screen digitizing methods according to the on-site installation time. Then, we visually identified the post-construction roads and foundation areas paving for wind transportations and installations and mapped the permanent land occupations and their boundaries using polygon tool in Google Earth Pro (version 7.3.4.8248) to estimate the land occupied by wind farm construction. Figure 7 shows the entire/partial remote sensed images of each wind farm, and the parts marked by the red lines are the permanent land occupation (including access roads, foundation clearing areas, cable areas all the paved surface area generated by wind power construction) by wind farms.

Data collection and inventory

The life cycle inventory data was developed based on multiple sources including Ecoinvent V3.8, manufacturers and previous studies (see Supplementary Table 2). Material consumption data for wind turbines were obtained from manufacturers or prior studies[31,51,52]. The GHG emission factors and energy data were derived from IPCC guidelines and corrected by recent studies of China[53–55].

Due to the high geographical dependence of wind energy, site-specific capacity factor and electricity production should be estimated based on accurate wind resource data with high temporal resolution[56]. Site-specific capacity factors and electricity generation were calculated using turbine power curves and hourly wind speed. The power curves were derived from manufacturers and the power curve database of Renewables.ninja[57] and hourly wind speed data were from MERRA-2 (M2I1NXLFO)[58] and Global Wind Atlas v2.0 (GWA v2). We conducted bias-correction for wind speed data using GWA v2. We first calculated the ratio between GWA v2's long-term wind speed values (V_{GWA2}) and 20-year mean wind speeds from each reanalysis dataset ($Mean_{MERRA\text{-}2}$ and $Mean_{ERA5\text{-}Land}$). Hourly wind speeds were then corrected using the

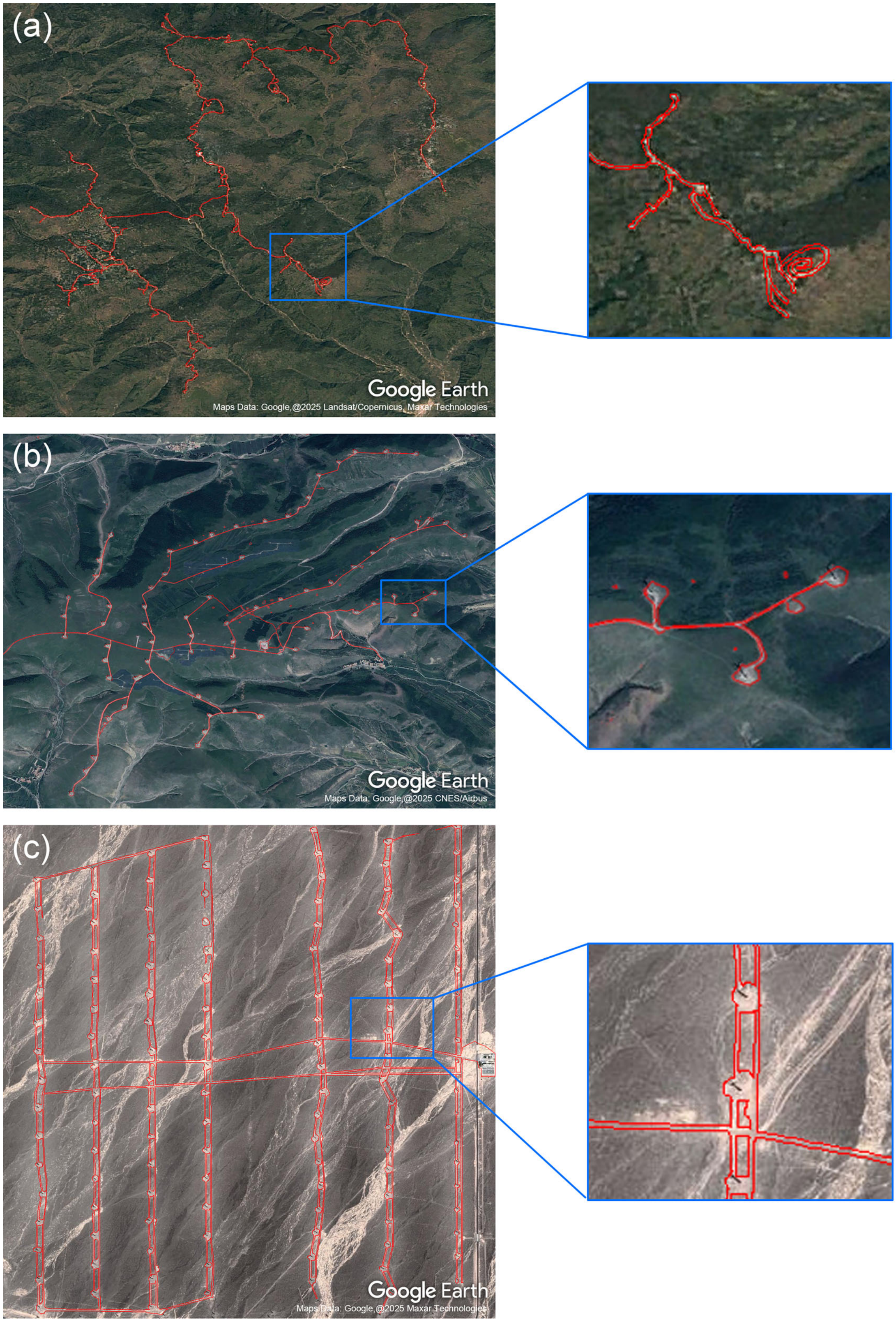

Fig. 7 | Geographical overview and land occupation of the studied wind farms. The left column represents the geographical overview of the three wind farms: **a** FWF, **b** GWF, and (**c**) DWF. The right column represents a magnified view of the wind farms. The red lines overlaid on the images represent the areas of permanent land occupation associated with each wind farm's infrastructure. The satellite images were sourced from Google Earth Pro (version 7.3.4.8248).

following equation:

$$V_{\text{MERRA-2 corrected}} = V_{\text{MERRA-2}} * V_{\text{GWA2}}/\text{Mean}_{\text{MERRA-2}} \quad (1)$$

$$V_{\text{ERA5-Land corrected}} = V_{\text{ERA5-Land}} * V_{\text{GWA2}}/\text{Mean}_{\text{ERA5-Land}} \quad (2)$$

The corrected hourly wind speed was then used to calculated the corrected capacity factor (*cf*) of each turbine.

Estimates of land-use change emissions were modeled using the CENTURY process-based model. The CENTURY model was first run to reach a steady-state where SOC input from vegetation and litter equal to the SOC loss from mineralization. Then the carbon input to soil was set to 0 and the model was run for 20 years. Considering the ecological succession after construction, we simulated the offsetting of grassland plants in the second year of the overall life cycle. Subsequently, productivity recovered to 50% (with ANPP and BNPP recovering from 0 to 50% between the second and sixth years). For FWF, based on remote sensing images indicating the long-term presence of paved road surfaces for transportation purposes, vegetation restoration was not factored into the CENTURY model. Similarly, for DWF, due to the slow restoration of perennial vegetation and low biomass, vegetation restoration was also not considered. Inputs for vegetation carbon density were derived from Global Aboveground and Belowground Biomass Carbon Density Maps in 2010[59], and soil organic carbon densities (SOCD) are from the Soil Database of China for Land Surface Modeling[60].

LASC drew on measured net ecosystem production (NEP) or net ecosystem exchange (NEE) of in-situ ecosystems from previous studies. For the Shaobaishan FWF, this was 311.72 g C m^{-2} y^{-1}, following Cai et al.'s results on forest NEP in northeastern China[61]. For Dongshan GWF, this was 78.89 g C m^{-2} y^{-1} grassland NEE from a nearby flux tower (Duolun Restoration Ecology Experimentation and Demonstration Station of China FLUX). For Guazhou Qiaowan DWF, this was 18.52 g C m^{-2} y^{-1} Gobi ecosystem NEE measured using the eddy covariance systems[62]. These mean annual NEP/NEE values were used to estimate the LASC in the entire operation and maintenance stage.

Impact assessment

Key metrics calculated include LUC induced GHG emissions and materials/energy use (t/t CO_2-eq), emission intensity (g CO_2-eq kWh^{-1}), land-use footprint (m^2 GWh^{-1}), EROI and EPT (month).

The LUC induced GHG emissions include biomass carbon loss ($CL_{biomass}$) from vegetation removal, SOC losses due to land occupation, and the loss of additional carbon sink capacity from land conversion. Biomass carbon loss ($CL_{biomass}$) was estimated by multiplying direct land area occupied (A) by the carbon density of the existing vegetation ($CD_{biomass}$).

$$CL_{biomass} = A \times CD_{biomass} \quad (3)$$

The SOC loss (CL_{soc}) over 20 years was modeled using the CENTURY process-based model, by running a simulation with zero carbon input to the soil after wind farm construction.

$$CL_{soc} = A \times \left(SOCD_0 - SOCD_{20}\right) \quad (4)$$

The biomass and SOC losses were converted to equivalent GHG emissions (GHG_{CS}) using their relative molecular masses. The loss of additional carbon sink capacity was also estimated (GHG_{LASC}), based on the assumed 20-year lifetime of the wind farm. This equals the NEP value of the original ecosystem multiplied by the area A and the lifetime.

The overall GHG emissions (GHG_{total}) include GHG_{CS}, GHG_{LASC}, and the emissions from materials and energy used in turbine construction, transportation etc. (i.e., GHG_M).

$$GHG_{total} = GHG_M + GHG_{CS} + GHG_{LASC} \quad (5)$$

The GHG emission intensity per kWh (GHG_{int}) was derived from the GHG_{total} divided by the estimated total power generation (*PG*) over 20 years. The *PG* among the entire life cycle was calculated as the product of the *cf*, nominal power of turbine (*P*), and lifetime

$$PG = 8760 \times 20 \times cf \times P \quad (6)$$

In addition, accounting for the potential decline in wind turbine performance, the calculated *cf* values of wind farms were estimated to decrease by 0.53% per year following the mean value from global studies on wind turbine performance decline (Supplementary Table 3). The detailed calculation of hourly *cf* and construction of aggregate power curve were detailed in Supplementary Methods 1.3.1. Land-use footprint and capacity density accounts for the requirement of direct occupation area per unit of wind power generation and direct occupation area that is needed to support per unit installed capacity, respectively. EROI and EPT compared total energy outputs from *PG* to inputs over the full wind farm life cycle. Detailed calculations and details are provided in the Supplementary Methods 1.3.

Result interpretation

Result interpretation of life cycle assessment integrates inventory analysis, impact assessment and the LCA goal to reach robust conclusions. We employed three additional analyses: decomposition analysis to parse out the specific impacts of factors like LUC and wind characteristics on overall results; sensitivity analysis to gauge uncertainty and parameter importance; and scenario analysis to explore mitigation potential of different solutions.

GHG emission intensity and EROI among the wind farms are affected by turbine model, wind regime and ecosystem type. We isolated the effect of each factor by fixing it between two farms through factorial simulations. Specifically, holding turbines identical between wind farms could reveal turbine-related differences in the GHG emission intensity and EROI, while using uniformed wind speed directly examined the impacts due to wind resource. Similarly, keeping identical LUC induced emissions between wind farms distinguished the impacts from ecosystem differences. This elucidated the relative contributions of these parameters.

Factors such as turbine size, life time, types of turbine, capacity factor, energy production, and transport distance are often considered in sensitivity analysis of previous wind LCAs[63]. We conducted sensitivity analysis using both: (1) location-specific capacity factors from existing wind farms, and (2) systematic ±20% parameter variations with a Monte Carlo simulation in key factors including capacity factor, consumption of different materials (divided into three parts: steel & iron, cement and other materials), life time, land-use area, transport distance, curtailment rate, and ecosystem. Geographic location was the most important factor affecting the energy performance and emission intensity; thus, we considered the potential variance of wind resource and conduct the uncertainty analysis. We examined all China's wind farms with same land type to the three wind farms we selected, aiming to calculate the variation in wind capacity across different regions[64]. Wind turbines and wind farms within a 1 km radius were aggregated into one wind farm, and we have identified a total of 128 forest wind farms, 141 grassland wind farms, and 124 desert wind farms. We applied the same bias-corrected method (following Eqs. (1) and (2)) to calculated the corrected capacity factors. These capacity factors, derived from these geographically representative wind farms, were further used as inputs in the LCA model to quantify the uncertainty ranges for the three selected wind farms. Considering the variance of SOC and biomass across different ecosystems, we simulated the 20-year SOC loss and estimated the biomass loss attributable to the installation and operation stage of the 493 wind farms China (see Methods section Impact assessment). The resulting uncertainties in SOC and biomass changes were systematically incorporated into the Ecosystem uncertainty category. To assess the uncertainty of other factors including material consumption, life time, land-use area, transport distance and curtailment rate, ±20% changes in key factors and assumptions combined with Monte Carlo simulation were applied to the LCA modeling. The probability distributions of input parameters in the Monte Carlo simulation were determined based on previous research and database[65–67] (see Supplementary Methods 1.4 for details).

Seven scenarios were designed in the study to explore the mitigation potential of wind farms including (1) Lifetime prolonging scenario ($S_{lifetime}$), (2) Advanced manufacturing scenario ($S_{advanced}$); (3) Clean manufacturing scenario (S_{clean}); (4) Recycling and reuse scenario ($S_{recycling}$); (5) Land reclamation scenario (S_{land}); (6) Reduced curtailment scenario ($S_{curtailment}$); (7) Large-scale (6 MW) turbine deployment scenario (S_{6MW}). Detailed information of scenario design was provided as follows.

$S_{lifetime}$. Wind turbines are conventionally designed for a lifetime of 20–25 years. In this scenario, the lifetime was assumed to reach 25.4 years following the maximum lifetime expectancy (95% CI) of Denmark's wind turbines under scrapping schemes[68]. The annual inputs and outputs of extended service in operation longer than the design lifetime were assumed to be the same as that within the designed lifetime span.

$S_{advanced}$. In this scenario, the main materials of wind facilities were assumed to be produced using advanced manufacturing technologies, while the emission factors and energy consumption factors were further reduced. Specifically, (1) a larger share of steel production using electric arc furnaces (~ 70%) with the GHG emission factor dropped to the Mexican level[69]; (2) iron was produced using direct reduced iron technology (following default assumptions in the 2006 IPCC guidelines); (3) copper was produced using secondary production copper[54]; (4) aluminum was produced using secondary production aluminum with the GHG emission factor dropped to the European level[70]; (5) silica was produced using continuous bioinspired processes[71]; (6) cement was produced from cement-based waste materials (clinker-to-cement ratio: 57%)[72,73].

S_{clean}. In this scenario, the electricity consumption in the manufacturing stage was assumed to be produced from wind power instead of coal-fired power (with a GHG emission factor of 800 g CO_2-eq·kWh^{-1} in the baseline scenario[69]). The emission factor of wind energy was used here following the national average in 2019 (19.88 g CO_2-eq·kWh^{-1})[4]. As a result, over 16% of the GHG emissions of manufacturing stage could be further reduced.

$S_{recycling}$. In contrast to the assumption of all vegetation losses as CO_2 emissions in the baseline scenario, the felled trees due to the construction of wind facilities in the forest ecosystem (the FWF) in this scenario was assumed to be further recycled for wood products. Foliage and fruit mass of trees were not reused (the same as that in baseline solution), while stem mass was recycled and used for further wood products. The biomass allocation data to distinguish foliage, fruit, root and stem mass was from the dataset of global forests[74], and the water content and carbon content followed previous measurements[75] and IPCC default. For stem mass, we assumed that 87% of the stem mass was used for producing solid wood products (hardwood lumber) and 13% of that was used for manufacturing papers[76]. The displacement factor (tWHP/reducing tC) from meta-analysis[77,78] and energy consumptions of manufacturing hardwood products based on LCAs[79] were used to quantify the GHG mitigation contributions and energy inputs for manufacturing solid wood products. The GHG emission factor and energy consumption factor of China's paper products were used to estimate the emissions and energy inputs of wood recycling[80,81].

S_{land}. In this scenario, two-thirds of the land occupation areas were assumed to be reclaimed by soil with 30 cm depth. It is assumed that the soil covering work took 1 hour on the area of 0.005 ha using VOLVO EC60B 37.4 kW[82]. For the forest ecosystem, the restored area was further implemented a reforestation project, and the extra energy inputs and LASC was quantified in this scenario[83].

$S_{curtailment}$. It is assumed that the curtailment rate of wind generations would reduce to 0.5% with no transmission constraints due to increasing transmission capacity and the rapid development of pumped hydro storage and electric boilers[84].

S_{6MW}. In this scenario, the existing wind turbines at the three sites were assumed to be upgraded with large-scale wind turbines Vestas V150 - 6 MW onshore turbines. The material breakdown of the turbine was obtained from the comprehensive life cycle inventory provided by Vestas, which facilitated a thorough life cycle assessment report[85]. The impact of land-use changes caused by larger turbine spacing distances as larger wind turbines was estimated based on the rotor diameter[86] as follows:

$$\text{turbine spacing distance} = 0.39 * \text{rotor diameter}^{1.38} \quad (7)$$

Data availability

All data generated in the publication, as well as the data underlying the Figures, are available from the Figshare repository: https://doi.org/10.6084/m9.figshare.28598276. Detailed information on wind farms and wind turbines, along with the life cycle inventory data, are provided in Supplementary Tables 1, 2 in the Supplementary Information.

Code availability

The analysis code used for data processing, power curve calculation, capacity factor and carbon loss simulation, and LCA calculation is available from the Figshare repository: https://doi.org/10.6084/m9.figshare.28598276.

Received: 27 January 2024; Accepted: 25 September 2025;
Published online: 17 November 2025

References

1. CEC (China Electricity Council) China power sector annual development report 2021. 中国电力行业年度发展报告2021 (2021).
2. IEA (International Energy Agency) An energy sector road map to carbon neutrality in China. (2021).
3. EFC (Energy Foundation China) Synthesis Report 2020 on China's Carbon Neutrality. (2020).
4. Xu, K. et al. A comprehensive estimate of life cycle greenhouse gas emissions from onshore wind energy in China. *J. Clean. Prod.* **338**, 130683 (2022).
5. GWEC (Global Wind Energy Council) Global Wind Report 2021. (2021).
6. Xie, Z., He, J., Li, Z. & Zhang, X. China's long-term low-carbon development strategies and pathways: Comprehensive report. (2021).
7. Wang, C. et al. Mapping potentials and bridging regional gaps of renewable resources in China. *Renew. Sustain. Energy Rev.* **134**, 110337 (2020).
8. Wachs, E. & Engel, B. Land use for United States power generation: A critical review of existing metrics with suggestions for going forward. *Renew. Sustain. Energy Rev.* **143**, 110911 (2021).
9. Nøland, J. K., Auxepaules, J., Rousset, A., Perney, B. & Falletti, G. Spatial energy density of large-scale electricity generation from power sources worldwide. *Sci. Rep.* **12**, 20280 (2022).
10. Dupont, E., Koppelaar, R. & Jeanmart, H. Global available wind energy with physical and energy return on investment constraints. *Appl. Energ.* **209**, 322–338 (2018).
11. Diffendorfer, J. E., Dorning, M. A., Keen, J. R., Kramer, L. A. & Taylor, R. V. Geographic context affects the landscape change and fragmentation caused by wind energy facilities. *PeerJ* **7**, e7129 (2019).
12. Zhou, L. et al. Impacts of wind farms on land surface temperature. *Nat. Clim. Change* **2**, 539–543 (2012).
13. Zhou, L., Baidya Roy, S. & Xia, G. In Comprehensive Renewable Energy 165-188 (2022).
14. Armstrong, A., Waldron, S., Whitaker, J. & Ostle, N. J. Wind farm and solar park effects on plant-soil carbon cycling: uncertain impacts of

changes in ground-level microclimate. *Glob. Chang. Biol.* **20**, 1699–1706 (2014).
15. Thaxter, C. B. et al. Bird and bat species' global vulnerability to collision mortality at wind farms revealed through a trait-based assessment. *Proc. R. Soc. B* **284**, 20170829 (2017).
16. Thompson, M., Beston, J. A., Etterson, M., Diffendorfer, J. E. & Loss, S. R. Factors associated with bat mortality at wind energy facilities in the United States. *Biol. Conserv.* **215**, 241–245 (2017).
17. Arvesen, A. & Hertwich, E. G. Assessing the life cycle environmental impacts of wind power: A review of present knowledge and research needs. *Renew. Sustain. Energy Rev.* **16**, 5994–6006 (2012).
18. Shen, G. et al. Monitoring wind farms occupying grasslands based on remote-sensing data from China's GF-2 HD satellite—A case study of Jiuquan city, Gansu province, China. *Resour. Conserv. Recycl.* **121**, 128–136 (2017).
19. Tang, B. et al. The Observed Impacts of Wind Farms on Local Vegetation Growth in Northern China. *Remote Sens.* **9**, 332 (2017).
20. Qin, Y. et al. Impacts of 319 wind farms on surface temperature and vegetation in the United States. *Environ. Res. Lett.* **17**, 024026 (2022).
21. Pekkan, O. I. et al. Assessing the effects of wind farms on soil organic carbon. *Environ. Sci. Pollut. Res.* **28**, 18216–18233 (2021).
22. Yeh, S. et al. Land Use Greenhouse Gas Emissions from Conventional Oil Production and Oil Sands. *Environ. Sci. Technol.* **44**, 8766–8772 (2010).
23. Zhang, B., Zhang, R., Li, Y., Wang, S. & Xing, F. Ignoring the Effects of Photovoltaic Array Deployment on Greenhouse Gas Emissions May Lead to Overestimation of the Contribution of Photovoltaic Power Generation to Greenhouse Gas Reduction. *Environ. Sci. Technol.* **57**, 4241–4252 (2023).
24. Fargione, J., Hill, J., Tilman, D., Polasky, S. & Hawthorne, P. Land clearing and the biofuel carbon debt. *Science* **319**, 1235–1238 (2008).
25. Taheripour, F., Zhao, X. & Tyner, W. E. The impact of considering land intensification and updated data on biofuels land use change and emissions estimates. *Biotechnol. Biofuels* **10**, 191 (2017).
26. Zhang, N. et al. Booming solar energy is encroaching on cropland. *Nat. Geosci.* **16**, 932–934 (2023).
27. Harrison-Atlas, D., Lopez, A. & Lantz, E. Dynamic land use implications of rapidly expanding and evolving wind power deployment. *Environ. Res. Lett.* **17**, 044064 (2022).
28. Augustyn, G., Mikulik, J., Rumin, R. & Szyba, M. Energy self-sufficient livestock farm as the example of agricultural hybrid off-grid system. *Energies* **14**, 7041 (2021).
29. Weidner, T., Yang, A., Forster, F. & Hamm, M. W. Regional conditions shape the food–energy–land nexus of low-carbon indoor farming. *Nat. Food* **3**, 206–216 (2022).
30. Amponsah, N. Y., Troldborg, M., Kington, B., Aalders, I. & Hough, R. L. Greenhouse gas emissions from renewable energy sources: A review of lifecycle considerations. *Renew. Sustain. Energy Rev.* **39**, 461–475 (2014).
31. Gao, C. et al. Environmental impact analysis of power generation from biomass and wind farms in different locations. *Renew. Sustain. Energy Rev.* **102**, 307–317 (2019).
32. Grodsky, S. M. & Hernandez, R. R. Reduced ecosystem services of desert plants from ground-mounted solar energy development. *Nat. Sustain.* **3**, 1036–1043 (2020).
33. Lovich, J. E. & Bainbridge, D. Anthropogenic Degradation of the Southern California desert ecosystem and prospects for natural recovery and restoration. *Environ. Manag.* **24**, 309–326 (1999).
34. Bingöl, F. A simplified method on estimation of forest roughness by use of aerial LIDAR data. *Energy Sci. Eng.* **7**, 3274–3282 (2019).
35. Meier, P. H. Wind farms adapt to forest conditions. https://www.renewableenergyworld.com/wind-power/wind-farms-adapt-to-forest-conditions (2011).
36. Diffendorfer, J. E. & Compton, R. W. Land cover and topography affect the land transformation caused by wind facilities. *PLoS One* **9**, e88914 (2014).
37. Dai, T. & Scown, C. D. A novel approach for large-scale wind energy potential assessment. *Renew. Sustain. Energy Rev.* **211**, 115333 (2025).
38. Kaffine, D. T. Microclimate effects of wind farms on local crop yields. *J. Environ. Econ. Manag.* **96**, 159–173 (2019).
39. Ding, Y. Launching the "Thousands of townships and tens of thousands of villages harnessing the wind program" to Explore a New Model of Village-Enterprise Cooperative Investment and Construction – Promoting the Development of Wind Power in Rural Areas in Light of Local Conditions (Policy Interpretation). 开展"千乡万村驭风行动", 探索村企合作投资建设新模式——推动农村因地制宜发展风电(政策解读). *People's Daily.* https://www.gov.cn/zhengce/202404/content_6943561.htm (2024).
40. Xin Hua News Agency. A Batch of Local Wind Power Projects to Be Built in Rural Areas of Counties in China. 我国将在县域农村建成一批就地就近的风电项目. https://www.gov.cn/lianbo/bumen/202404/content_6942962.htm (2024).
41. Hubner, G. et al. Monitoring annoyance and stress effects of wind turbines on nearby residents: A comparison of U.S. and European samples. *Environ. Int.* **132**, 105090 (2019).
42. Radun, J., Hongisto, V. & Suokas, M. Variables associated with wind turbine noise annoyance and sleep disturbance. *Build. Environ.* **150**, 339–348 (2019).
43. Xia, G. & Zhou, L. Detecting Wind Farm Impacts on Local Vegetation Growth in Texas and Illinois Using MODIS Vegetation Greenness Measurements. *Remote Sens.* **9**, 698 (2017).
44. Luo, L. et al. Local climatic and environmental effects of an onshore wind farm in North China. *Agric. For. Meteorol*. **308-309** (2021).
45. Li, Y. et al. Climate model shows large-scale wind and solar farms in the Sahara increase rain and vegetation. *Science* **361**, 1019–1022 (2018).
46. Xu, K. et al. Positive ecological effects of wind farms on vegetation in China's Gobi desert. *Sci. Rep.* **9**, 6341 (2019).
47. Laranjeiro, T., May, R. & Verones, F. Impacts of onshore wind energy production on birds and bats: recommendations for future life cycle impact assessment developments. *Int. J. Life Cycle Assess.* **23**, 2007–2023 (2018).
48. Li, C. et al. Offshore Wind Energy and Marine Biodiversity in the North Sea: Life Cycle Impact Assessment for Benthic Communities. *Environ. Sci. Technol.* **57**, 6455–6464 (2023).
49. Chen, Y. et al. Changes in soil carbon pools and microbial biomass from urban land development and subsequent post-development soil rehabilitation. *Soil Biol. Biochem.* **66**, 38–44 (2013).
50. Yang, G. et al. Identifying the greenhouses by Google Earth Engine to promote the reuse of fragmented land in urban fringe. *Sustain. Cities Soc.* **67**, 102743 (2021).
51. Xu, L., Pang, M., Zhang, L., Poganietz, W.-R. & Marathe, S. D. Life cycle assessment of onshore wind power systems in China. *Resour. Conserv. Recycl.* **132**, 361–368 (2018).
52. Li, L., Ma, X., Xie, M. & Liao, Y. Full Life Cycle Assessment on Wind Power Generation System. 风力发电系统的全生命周期分析. (in Chinese with English abstract). *Chin. J. Turbomach.* **2**, 65–70+84 (2015).
53. Meng, F. et al. Comparing Life Cycle Energy and Global Warming Potential of Carbon Fiber Composite Recycling Technologies and Waste Management Options. *ACS Sustain. Chem. Eng.* **6**, 9854–9865 (2018).
54. Dong, D., van Oers, L., Tukker, A. & van der Voet, E. Assessing the future environmental impacts of copper production in China: Implications of the energy transition. *J. Clean. Prod*. **274**, 122825 (2020).
55. Geng, Y., Wang, Z., Shen, L. & Zhao, J. Calculating of CO2 emission factors for Chinese cement production based on inorganic carbon and organic carbon. *J. Clean. Prod.* **217**, 503–509 (2019).

56. Poujol, B. et al. Site-specific life cycle assessment of a pilot floating offshore wind farm based on suppliers' data and geo-located wind data. *J. Ind. Ecol.* **24**, 248–262 (2020).
57. Staffell, I. & Pfenninger, S. Using bias-corrected reanalysis to simulate current and future wind power output. *Energy* **114**, 1224–1239 (2016).
58. Molod, A., Takacs, L., Suarez, M. & Bacmeister, J. Development of the GEOS-5 atmospheric general circulation model: evolution from MERRA to MERRA2. *Geosci. Model. Dev.* **8**, 1339–1356 (2015).
59. Spawn, S. A. & Gibbs, H. K. Global Aboveground and Belowground Biomass Carbon Density Maps for the Year 2010. ORNL Distributed Active Archive Center. (2020).
60. Shangguan, W. et al. A China data set of soil properties for land surface modeling. *J. Adv. Model Earth Syst.* **5**, 212–224 (2013).
61. Cai, H. et al. Carbon storage, net primary production, and net ecosystem production in four major temperate forest types in northeastern China. *Can. J. Res.* **46**, 143–151 (2016).
62. Zhang, L., Sun, R., Xu, Z., Qiao, C. & Jiang, G. Diurnal and seasonal variations in carbon dioxide exchange in ecosystems in the Zhangye oasis area, Northwest China. *PLoS One* **10**, e0120660 (2015).
63. Alsaleh, A. & Sattler, M. Comprehensive life cycle assessment of large wind turbines in the US. *Clean. Technol. Environ. Policy* **21**, 887–903 (2019).
64. Dunnett, S., Sorichetta, A., Taylor, G. & Eigenbrod, F. Harmonised global datasets of wind and solar farm locations and power. *Sci. Data* **7**, 130 (2020).
65. Bech Abrahamsen, A. et al. Method for estimating the future annual mass of decommissioned wind turbine blade material in Denmark. *Wind Energy* **27**, 165–178 (2023).
66. Ruan, Z. et al. Spatiotemporal carbon footprint and associated costs of wind power toward China's carbon neutrality. *Resour. Conserv. Recycl* **205**, 107593 (2024).
67. Yang, N. et al. Land-use requirements and occupancy patterns of rapidly expanding wind power deployment in China. *Environ. Res. Lett*. **20**, 074011 (2025).
68. MEGAVIND. Strategy for Extending the Useful Lifetime of a Wind Turbine. 66. (2016)
69. Hasanbeigi, A., Arens, M., Cardenas, J. C. R., Price, L. & Triolo, R. Comparison of carbon dioxide emissions intensity of steel production in China, Germany, Mexico, and the United States. *Resour. Conserv. Recycl.* **113**, 127–139 (2016).
70. Zhang, Y. et al. Environmental footprint of aluminum production in China. *J. Clean. Prod.* **133**, 1242–1251 (2016).
71. Drummond, C., McCann, R. & Patwardhan, S. V. A feasibility study of the biologically inspired green manufacturing of precipitated silica. *Chem. Eng. J.* **244**, 483–492 (2014).
72. Wei, J. & Cen, K. Empirical assessing cement CO2 emissions based on China's economic and social development during 2001−2030. *Sci. Total Environ.* **653**, 200–211 (2019).
73. Sousa, V. & Bogas, J. A. Comparison of energy consumption and carbon emissions from clinker and recycled cement production. *J. Clean. Prod.* **306**, 127277 (2021).
74. Michaletz, S. T., Cheng, D., Kerkhoff, A. J. & Enquist, B. J. Convergence of terrestrial plant production across global climate gradients. *Nature* **512**, 39–43 (2014).
75. Dias, D. P. & Marenco, R. A. Tree growth, wood and bark water content of 28 Amazonian tree species in response to variations in rainfall and wood density. *iForest* **9**, 445–451 (2016).
76. Zhang, L., Sun, Y., Song, T. & Xu, J. Harvested Wood Products as a Carbon Sink in China, 1900−2016. *Int. J. Environ. Res. Public Health* **16**, 445 (2019).
77. Sathre, R. & O'Connor, J. Meta-analysis of greenhouse gas displacement factors of wood product substitution. *Environ. Sci. Policy* **13**, 104–114 (2010).
78. Geng, A., Yang, H., Chen, J. & Hong, Y. Review of carbon storage function of harvested wood products and the potential of wood substitution in greenhouse gas mitigation. *Policy Econ.* **85**, 192–200 (2017).
79. Bergman, R. D. & Bowe, S. A. Life-cycle inventory of manufacturing hardwood lumber in southeastern US. *Wood Fiber Sci.* **44**, 71–84 (2012).
80. Chen, S., Yang, X., Li, Y., Cao, L. & Yue, W. Life-cycle GHG Emissions of Paper in China. 中国纸产品全生命周期GHG排放分析. (in Chinese with English abstract). *J. Beijing Univ. Technol.* **40**, 944–949 (2014).
81. Zhao, G., You, Y. & Huang, Q. Carbon Footprint Assessment Method of Corrugated Medium on Life Cycle Assessment. 基于生命周期评价的瓦楞原纸产品碳足迹评价. (in Chinese with English abstract). *China Pulp. Pap.* **40**, 40–44 (2021).
82. Qu, L. et al. Characteristics of PM2. 5 emissions and its carbonaceous components from construction machines under different typical driving modes. *Res. Environ. Sci.* **28**, 1047–1052 (2015).
83. Lefebvre, D. et al. Assessing the carbon capture potential of a reforestation project. *Sci. Rep.* **11**, 19907 (2021).
84. Jorgenson, J., Mai, T. & Brinkman, G. Reducing wind curtailment through transmission expansion in a wind vision future. *NREL.* https://docs.nrel.gov/docs/fy17osti/67240.pdf (2017).
85. Vestas. Life Cycle Assessment of Electricity Production from an onshore EnVentus V150-6.0 MW Wind Plant - 31st January 2023. Vestas Wind Systems A/S, Hedeager 42, Aarhus N, 8200, Denmark (2022).
86. Dai, T. et al. Land resources for wind energy development requires regionalized characterizations. *Environ. Sci. Technol.* **58**, 5014–5023 (2024).

Acknowledgements

This work is supported by the National Natural Science Foundation of China (NSFC) (Grant No. 42401326, 32222053, 32361143871) and the Wuxi University Research Start-up Fund for Introduced Talents (2023r031).

Author contributions

K.X., H.Z. and J.C. conceived the study. K.X., H.Z., S.Z., M.W. and J.C. performed the analysis. K.X., H.Z., W.L., W.Z., S.L., Z.S. and J.C. contributed data interpretation and wrote the paper. K.X., S.Z., M.W. and J.C. designed and conducted simulations. K.X. and H.Z. performed dataset preparations. All authors contributed to the discussion and final version of the paper.

Competing interests

The authors declare no competing interests.

Additional information

Supplementary information The online version contains supplementary material available at https://doi.org/10.1038/s43247-025-02833-w.

Correspondence and requests for materials should be addressed to Jinfeng Chang.

Peer review information *Communications Earth and Environment* thanks Johannes Schmidt, Sabrina Spatari and the other, anonymous, reviewer(s) for their contribution to the peer review of this work. Primary Handling Editors: Martina Grecequet. [A peer review file is available].